International Journal on Recent and Innovation Trends in Computing and Communication
ISSN: 2321-8169 Volume: 11 Issue: 2
DOI: https://doi.org/10.17762/ijritcc.v11i2.6131
***Article Received**: 18 December 2022 **Revised**: 12 January 2023 **Accepted**: 24 January 2023*

Condition based Ensemble Deep Learning and Machine Learning Classification Technique for Integrated Potential Fishing Zone Future Forecasting

R Vinston Raja[1], Dr. K. Ashok Kumar[2], Dr. V. Gokula Krishnan[3]
[1]Research Scholar, School of Computing
Sathyabama Institute of Science and Technology
Chennai, Tamil Nadu, India
e-mail: rvinstonraja@gmail.com
[2]Associate Professor, School of Computing
Sathyabama Institute of Science and Technology
Chennai, Tamil Nadu, India
e-mail: ashokkumrk.cse@gmail.com
[3]Professor, Department of CSE, Saveetha School of Engineering
Saveetha Institute of Medical and Technical Sciences
Thandalam, Chennai, Tamil Nadu, India
e-mail: gokul_kris143@yahoo.com

Abstract— Artificial Intelligence (AI) technologies have become a popular application in order to improve the sustainability of smart fisheries. Although the ultimate objective of AI applications is often described as sustainability, there is yet no proof as to how AI contributes to sustainable fisheries. The proper monitoring of the longitudinal delivery of different human impacts on activities such as fishing is a major concern today in aquatic conservation. The term "potential fishing zone" (PFZ) refers to an anticipated area of any given sea where a variety of fish may congregate for some time. The forecast is made based on factors including the sea surface temperature (SST) and the sea superficial chlorophyll attentiveness. Fishing advisories are a by-product of the identification procedure. Normalization and preliminary processing are applied to these unprocessed data. The gathered attributes, together with financial derivatives and geometric features, are then utilised to make projections about IPFZ's Technique are used to get the final determination (CECT). In this study, we offer a technique for identifying and mapping fishing activity. Experimentations are performed to validate the efficacy of the CECT method in comparison to machine learning (ML) and deep learning (DL) methods across a variety of measurable parameters. Results showed that CECT obtained 94% accuracy, while Convolutional neural network only managed 92% accuracy on 80% training data and 20% testing data.

Keywords- Artificial Intelligence, Machine Learning, Classification Procedure, Convolutional Neural Network, Financial Derivatives Features, Potential Fishing Zone.

I. INTRODUCTION

The use of artificial intelligence technology in smart fisheries[1–2] is a point of reference for a number of stakeholders to tackle the diminishing fish stock[3] problem. Since 2018, the UN, the EU and the national governments have drawn up their IA agendas announcing a so-called new 'AI age'[4]. The UN has had its Good Series AI at world governance level since 2017. AI's assessment of opportunities to promote UN Sustainable Development Goals (SDGs) was set out on this platform and to ensure that the SDGs help all humanities. The AI Good series of the United Nations is based on the conviction that AI is a beneficent power that can solve humanity's intractable issues, including marine habitat deterioration and fish shrinkage. The EU AI Approach and the national AI Approaches convey similar thoughts. AI is positioned in these concerted policies as the benign force that resolves the problem of the ecosystem [5], among other things.

During the last decade, smart fishing literature has advanced greatly in our understanding of AI skills in PFZ in particular on key elements of optimization of resource efficiency in ecosystem management [6]. Automated classification is a prominent subject in various articles [7-8]. In fish categorization methods, AI technology is applied in automation. Some papers focus on systems for fish detection. These systems are built on profound network topologies to notice and count fish items robustly below a diversity of benthic settings and lighting [9-10]. In fact, these automation themes have the same results, albeit there are super laps between the categorization, detection and identification of fish stocks. For observing of the quality and health of fish containers, data on the composition of species and on the

International Journal on Recent and Innovation Trends in Computing and Communication
ISSN: 2321-8169 Volume: 11 Issue: 2
DOI: https://doi.org/10.17762/ijritcc.v11i2.6131
***Article Received**: 18 December 2022 **Revised**: 12 January 2023 **Accepted**: 24 January 2023*

distribution of abundance of fish species are important[11-12]. Smart fisheries as a resource categorization, identification and detection are included in the automatic perspective for evaluating fish abundance. A studies examined noted, fish abundance is the world's and national fishing industry's most unsustainable reasons[13]. AI-inspired sustainable smart fisheries are not just tied to fish stock surveillance in the studies examined.

The smart fishing scope in Kylili et al [14] (pp. 42632) emergency measures are necessary to prevent the decline of fish stocks from being pursued in a plastics epidemic.' They show that pollution is an urgent and essential factor in the abundance of fish. Oils also have a detrimental impact on aquatic and wild animals on seas and oceans [15-16] — a key source of pollution from the sea and oceans due to anthropogenic activity and the increasing demand for petroleum and marine transport volume. Song et al., [17] share this understanding, which suggests that sea oil spills generally lead to major marine contamination and gravely damage marine ecosystems, the environment and fishing. Moreover, an increase in global surface temperature urgently requires studying the influence on fisheries of future climate change[18].

In this research, CECT technology is used to estimate the IPFZ for the future, as described in the suggested part. The missing techniques to extract financial derivatives from the input data as well as the collected attributes. The ultimate prediction of PFZ is based on the ensemble ML and DL approach. The rest of the paper has been prearranged: Section 2 shows its limitations on the connected works. Section 3 delivers a explanation of the methods proposed. Section 4 describes the validation of the methodology presented with its present techniques. Finally, Section 5 presents the conclusion of the research with its future work.

II. Related Works

ANN training and testing procedures were presented by Cabreira et al[19] for the automatic credit and organization of South West Atlantic digital echo-recording in schools. The ANNs were supposed to be supplied with energetic, and bathymetric school description from echo records. Levelling the input data by species obtained the best outcome. Contingent on the species, kind of network and sum of school forms used, correct rates were touched up to 96 percent. Further this approach as a useful tool to examine echograms was suggested.
A self-representing wavelet model using the hybrid less square (LS) approach was developed by Rodriguez et al [20] and a one month Forecast Algorithm for Marquardt (LM+LS) of Levenberg, for monthly catches. Monthly data from sardines were initially divided in half using an un-decimated stationary wavelet treatment. Inputs for the proposed model for forecasting and the creation of new monthly sardines were derived from the relevant sub-series. The forecast performance based on (LM+LS) algorithms was assessed with a coefficient of determination and revealed that 99% of the variance explanation was accurately recorded.

The radial basis neural network model for prognostication fisheries has been created by Shakya et al.[21] and employs the Argentinean Illex southwest Atlantic as its testing grounds. The model initiates with the network factors for the perfect using ultimately with the test data set the forecasting outcomes. In this work, a total of six environmental elements are employed for the prediction of the A composite index of habitat quality and cumulative habitat length. Daily Production Index, which is derived from Total Habits Index, is one of the two indexes used to derive the final tally. Multiple linear regressions are utilized as a statistical model in fishing forecasts as well. The RBFNN model's output was compared to that of other regressions in terms of the accuracy metrics MSE, RAE, and PE. The smart model is proved to be highly predictive and fit with regard to statistical models.

The paper on PFZ in Makassar directly in Indonesia for Rastrelliger kanagurta has been provided by Nurdin et al[22]. Nurdin et al. Aqua/Terra MODIS concentration in SST and CHL along with fishing catch figures from 2008 and 2009 have been utilized to trace probable Rastrelliger kanagurtal fishing areas in Spermonde Indonesia archipelago waters. The determination of this study was to establish the preferred CHL and SST ranges for R. kanagurta and to identify their possible fishing estates on the basis of the marine factors. The pictures have been categorized with the preferred ranges by the appropriate scores and the prospective map has been integrated using GIS. The preferential range of CHL content was 0,31 ± 0,10 mg/m3 with the maximum catch of r. kanagurta and 29,94 ± 0,230 C for SST. Salleh et al[23] demonstrated the potential fishing plan for a MODIS seasonal distribution of salt sea (SSS), SST, and CHL in the sea waters off Semporna's coast, Malaysia, using MODIS information. This study shows GIS maps are able to map possible maritime fishing grounds for R. kanagurta. Multilinear regression analysis was carried out to estimate the SSS, and the SST algorithms Brown and Minnet were applied. In situ measurement using the Hydro-Lab tackle the extracted parameters were checked. The parameters retrieved from MODIS pictures indicate the signature values that build correlations between these parameters and hence delineate the PFZ map. The Rô was calculated as 0.93 and the greater catch regions have very well matched the higher PFZ values. This means that the technique is ready to be used for near real-time predictions of fish.

Tadjuddah and others [24] studied in the South-East of Sulawesi district of Wakatobi for the long-term objective of better fishing conditions, and the shorter-term objective is to

International Journal on Recent and Innovation Trends in Computing and Communication
ISSN: 2321-8169 Volume: 11 Issue: 2
DOI: https://doi.org/10.17762/ijritcc.v11i2.6131
***Article Received**: 18 December 2022 **Revised**: 12 January 2023 **Accepted**: 24 January 2023*

map the fishing ground for Yellow Fin tuna by applying multi-sensor satellite technology. The authors used the data from Topex-Poseidon satellite from MODIS SST & CHL and Sea Surface Height (SSH). The average marine surface temperature was 29.79 C in the west, 29.70 C in the east in the west, and 29.13 C in the east, in the east, in the East and in the East. CHL averaged approximately 0.15 mg m 3 in the West and Western countries, 0.27 mg m 3 in the East and 0.21 mg m 3 in the East West. Throughout December, high temperatures began and remained in the wakatobi area from west to east until February. From June through August, low temperatures migrated east to west. Finally, he mapped Thunnus albacores' fishing ground utilizing remote sensing and GIS technology employing markers like hot fronts, uplift and fish behavior in the area under research.

III. Proposed System

The following Figure 1 shows the working flow of proposed methodology. Initially, the collected (raw) data has unwanted and missing data, which should be removed by using normalization and pre-processing techniques. The financial derivatives features are extracted from the pre-processed data and these features are given to ensemble DL and ML techniques. These output labels are given to the condition checking for final decision label. The explanation of each process is given in detailed.

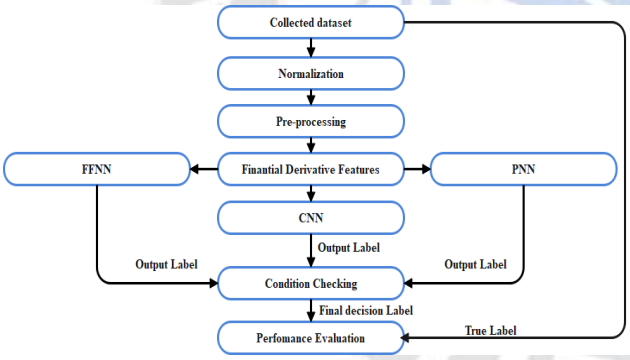

Figure 1: Proposed Architecture

3.1. Dataset

Met-OP satellites regularly gather Sea Surface Temperature (SST), chlorophyll, and Oceansat (US) data, which is then used to identify possible fishing zones around the Indian coastline. Advertisements for PFZs, in the form of PFZ Maps and PFZ Texts, are created for each individual sector (latitude and longitude information). Due to the fluid nature of the ocean, the selected location may be relocated when fishing hotspots are mapped out. The PFZ maps that are used to advise fishermen of impending changes in PFZ also include data on wind speed and direction. With this knowledge, fisherman can find the PFZ on maps; nevertheless, it will take them a whole day to get there. All PFZ maps and text are translated into the local languages for the benefit of fishermen. The PFZ text specifies the length and latitude of the PFZ site, as well as its depth and the distance from easily identifiable landmarks along the shore (a fishing landing centre and lighthouses, for example)..

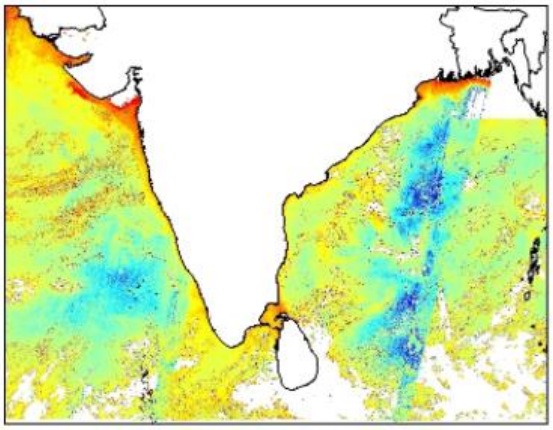

Figure 2: Chlorophyll Image retrieved from Oceansat-2 Satellite Data

3.2. Pre-processing & Normalization

Pre-processing methods are used to get rid of the extraneous data and fill in the gaps. During normalization, the data format is also changed. At the outset, we have 16 characteristics and a total of 151031 raw data points to work with. We use all of the raw data for training purposes, and the total sum of features is listed in Table 1.

Table 1: Feature Description

Description
LATITUDE_DEGREE
LATITUDE_MINUTE
Landing_Center (LC)
LONGITUDE_DEGREE
LONGITUDE_MINUTE
ANGLE
DISTANCE_FROM (DIF)
DISTANCE_TO (DIT)
LONGITUDE_SECOND
LONGITUDE_DIRECTION
DEPTH_FROM (DEF)
DEPTH_TO (DET)
LATITUDE_SECOND
LATITUDE_DIRECTION

The 16 components are The proposed model is trained using UPDATED DATE as the target data. The purpose is to anticipate the possible fisheries zone by providing future data, and the input data spans from2013, to 2018. Therefore, this study employs a total of 15 characteristics, however only 13 are employed throughout network training. Because the 151031

International Journal on Recent and Innovation Trends in Computing and Communication
ISSN: 2321-8169 Volume: 11 Issue: 2
DOI: https://doi.org/10.17762/ijritcc.v11i2.6131
***Article Received**: 18 December 2022 **Revised**: 12 January 2023 **Accepted**: 24 January 2023*

data includes redundant information in the feature, it cannot be used to train the proposed model. During pre-processing, the "-" is eliminated from between the dates so that the proposed network may train with cleaner data. In the DIRECTION function, you may choose from seven different compass points: south east (SE), south west (SW), north east (NE), south (S), east (E), north (N), and west (W) (W). These characters are turned into variables since they cannot be utilized directly in the training of the proposed model. Additionally, the Landing Center feature, which was originally in a floating format, has been converted to a double format for enhanced forecast accuracy. Therefore, the FFNN is fed input consisting of 13 characteristics in order to forecast the PFZ. This study takes into account the extra elements known as financial derivatives and geometrical aspects in order to provide accurate predictions about the future IPEZ. In what follows, I shall elaborate on these characteristics:

3.3. Financial Derivative Features

It's also important to think about how the data are handled, because it's rare for an algorithm to be given access to raw data values. Therefore, we need to adjust the information such that it fits within our issue domain. The goal of this study is to predict the IPFZ over the specified area using data on the total number of fish in the system. The requirement to close future contracts, typically up to a year in advance, is a crucial consideration, and the duration of the contracts themselves might be of any length. The necessity for data transformation is heightened further by the unique nature of the PFZ projections. Because of this, we use a Financial Derivative function to transform the information into a form better suited to the issue at hand. Financial derivatives are used to increase data fluidity and provide a result that seems to be considerably less manipulated. Additionally, daily volatility appears to be smaller, and a pattern is simpler to recognize in PFZ forecasting. The horizon for which this method of IPFZ prediction is used can be altered at will.

Table 2: List of Financial Unoriginal and Geometrical Topographies used

Financial Derivative Features
Modification of Least over Last Contract Distance
Modification of Extreme over Last Contract Distance
Autocorrelation
Mean Standard
Contrast
Deviation Sum
Correlation
Alteration Adjacent
Cluster Prominence
Difference Moving
Cluster Shade
Average Standard
Time Last Extreme
Sum variance
Energy
Last Supreme
Entropy
Last Smallest
Homogeneity
Supreme probability
Time Last Least
Magnitude of Least
Magnitude of Supreme
Minimum Last Contract Distance
Maximum Last Contract Distance
Dissimilarity
Deviation across MA

3.4. Classification

Here, we discuss an ensemble ML and DL approach utilized for last classification; ML techniques employed here comprise FFNN and PNN, while DL techniques used here include CNN.

3.4.1. Function Fitting Neural Network (FFNN)

A neural network includes several stages of processing, using components that are both fundamental and inspired by the nervous system of living organisms. It has an input layer, a few layer. As a result, neurons connect the various levels and are involved in the input of each layer. During learning, the weights of all neurons are adjusted, changing how much of an impact each neuron has on the network as its signal intensity increases or decreases. Fig. 1 explains the basic make-up of an FFNN. 3.

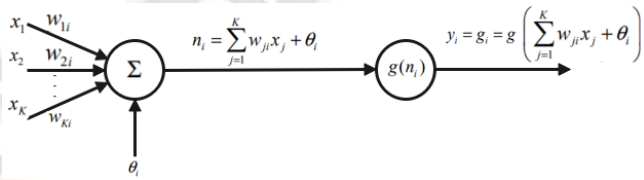

Figure 3: Single node in a FFNN system

Multiplying and adding the neuron's inputs x k,k=1,...k, and the constant bias term _i. Input enabling g will be done by the resultant n i. However, a sigmoid function or a hyberbolic tangent (tanh) is the most frequent activation function from the outset because to its mathematical simplicity. Hyperbolic is one definition of tangent.

$$\tanh(x) = \frac{1-e^{-x}}{1+e^{-x}} \quad (1)$$

The node i develops

International Journal on Recent and Innovation Trends in Computing and Communication
ISSN: 2321-8169 Volume: 11 Issue: 2
DOI: https://doi.org/10.17762/ijritcc.v11i2.6131
***Article Received**: 18 December 2022 **Revised**: 12 January 2023 **Accepted**: 24 January 2023*

$$y_i = g_i = g\left(\sum_{j=1}^{K} w_{ji} + x_j + \theta_i\right) \quad (2)$$

A FFNN network is constructed by serially and parallelly interconnecting several nodes. Figure 4 depicts a characteristic network layer.

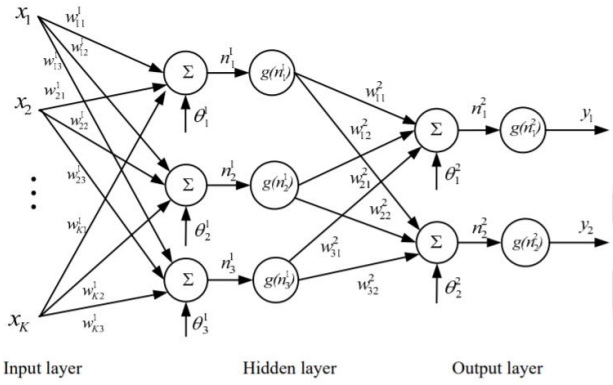

Figure 4: hidden layer FFNN

$$y_i = g\left(\sum_{j=1}^{3} w_{ji}^2 g(n_j^1) + \theta_j^2\right) = g\left(\sum_{j=1}^{3} w_{ji}^2 g\left(\sum_{k=1}^{K} w_{kj}^1 + \theta_j^1\right) + \theta_j^2\right) \quad (3)$$

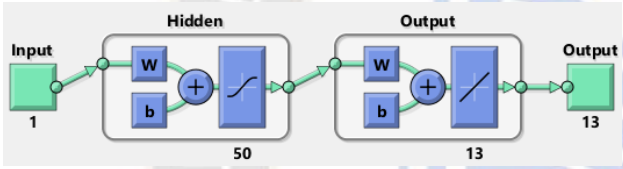

Figure 5: The Projected Matlab FFNN Construction

The post-processing is done once the FFNN outputs have been obtained. Here, the LC feature's double format is transformed into text. DIR's variables are shifted in seven different instructions. Thus, the output of the FFNN model will be presented in a suitable format, such as the place name, its direction, latitude, and longitude, should the user provide future data as input. The results of the suggested model's performance analysis are shown in the next section.

3.4.2. Probabilistic Neural Networks

To help understand how PNNs work, Parzen (1962) [25] noted that a family of estimators in the form of a sequence of PDF f(X) is projected with a random variable n X1, X2,...,Xn with unknown PDF f(X)..

$$f_n(x) = \frac{1}{nh(n)} \sum_{j=1}^{n} K\left(\frac{x - X_j}{h(n)}\right) \quad (4)$$

where h(n) is a arrangement of information that contents:

$$\lim_{n \to \infty} h(n) = 0 \quad (5)$$

However, K(y) is typically a Borel function that filling these conditions:

$$\sup_{-\infty < y < \infty} K(y) < \infty \quad (6)$$

$$\int_{-\infty}^{\infty} |K(y)| d_y < \infty \quad (7)$$

$$\lim_{y \to \infty} |yK(y)|\, d_y = 0 \quad (8)$$

$$\int_{-\infty}^{\infty} K(y) d_y = 1 \quad (9)$$

Then

$$\lim_{n \to \infty} E[f_n(x) - f(x)]^2 = 0 \quad (10)$$

Using Eq.(10), we see that X is n. The Parzen family of PDFs may be approximated using the n-diameter method. Readers interested in PNNs should learn more about Parzen (1962). according to [26] Specht (1990).

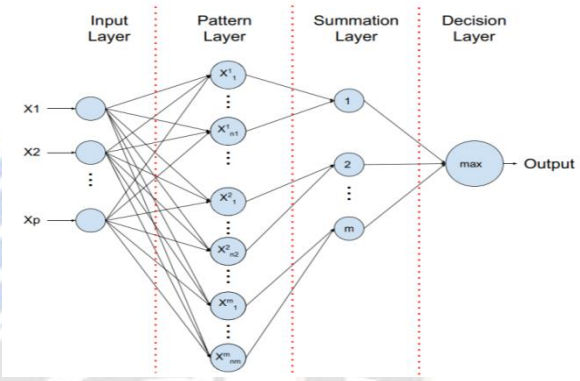

Figure 6: The basic construction of a network

To further understand how a PNN would tackle this problem, let's take a set of training data consisting of a series of independent random variable pairs, Xi, Yi, where Y i is the class associated with the pattern Xi A rather than R p. The order of applications is also taken into account. Xi is a random variable with an unknown probability dense function (f m) that is determined by the class f m (x), which is mentioned to as "class conditions" in [27]. (x).

The discriminating power of group j in the form of shadows:

$$d_j(x) = p_i f_i(x) \quad (11)$$

where p_j is signified as the prior likelihood of class j and is given by:

$$p_j = \frac{n_j}{n} \quad (12)$$

Where n is the total sum of models used during training and n j is the total sum of patterns fitting to class j. The density probability function, f i (x), is denoted by x. If we have an x pattern and know its class, we can write m.

$$d_m(x) > d_j(x)$$
$$\forall j \in \{1,2, \ldots M\}, j \neq m \quad (13)$$

International Journal on Recent and Innovation Trends in Computing and Communication
ISSN: 2321-8169 Volume: 11 Issue: 2
DOI: https://doi.org/10.17762/ijritcc.v11i2.6131
***Article Received**: 18 December 2022 **Revised**: 12 January 2023 **Accepted**: 24 January 2023*

Since f_j (x) is usually unidentified, its estimator. Using Eq. (14), we can approximation f_j (x) as follows:

$$\hat{f}_{j,n} = \frac{1}{h_{nj}^{p}} \sum_{i=1}^{n_j} K(x, X_i^{(j)}) \quad (14)$$

Assume X i((j)) is the ith design used to teach Class j. The size and shape of the vector inputs are denoted by p. Figure 6 depicts the underlying example of the current formulation. Input, pattern, summation, and decision layers make up the four-tiered structure of Specht's network (1990) [26].

To pass an input vector to the next layer, the layer's input is effectively a sequence of p-intersections. The majority of the plans are stored in the pattern layer. Each model in the training sequence has its own unique design unit that performs a two-step procedure to apply the input vector before passing on its consequence to the following layer. The initial process involves a comparison between the pattern and the input vector by the pattern unit. We have gone thus far in elucidating the potential roles. The distance between the input vector x and the ith pattern, X i((j)), is denoted as D(x, Xi((j)) in the training arrangement of class j.

What we mean by "Euclidean distance" is

$$D(x, X_i^{(j)} = \sum_{k=1}^{p} x_k . X_{i,k}^{(j)}) \quad (15)$$

3.4.3. One Dimensional Convolutional Neural Network

Layer combinations including a layer, and a fully linked layer are the most common building blocks of a typical CNN. Conv1, Conver2, Pool1, Pool2, and Fully Connected Layer make up the broad framework of a deep neural network, as seen in Figure 7.

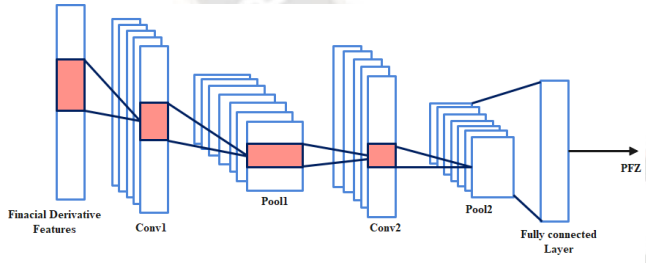

Figure 7. A common construction of --D CNN

The convolutionary layer is the main component of the neural network. The network layers are usually fully linked to all neurons of the preceding layer by the neuron in the next layer. Neurons are linked to the local regions of the preceding layer during convolutionary layers. In order to further determine effective predictors of IPFZ, we propose to leverage these types of connections. The structure of the convolutionary layer is affected by several parameters, including: filter size, filter sum, stride and padding. The filter dimension is the local field of reception, which is a space area over the vector. The convolutionary layer, as shown in Figure 7, is seen as a layer stack. Depending on the sum of filters you choose, the number of layers is decided. Stride affects the movement of the filter via input (local receptive field). Padding is a technique through which values are added/removed to the input dimension so that the filter can pass over the entire dimension.

Through its hierarchical layer structure is the convolutionary neural network. Deepening the layers improves the learning of complex input relations. The forecast model performance in the IPFZ prediction is reliant on the input characteristics. Input features = δ^1 ,δ^2 ,...,δ^n , 1 ⩽ i ⩽ n,n are the input features that can lead to greater performance when the input is sub-set β(β ⊂ δ) than the input feature is used. In the data set of input functionality, removal of the pieces can delete some of the information required to carry out the model. In addition, ^^1 can greatly alter the forecast of particular instances and may not be of use in other applications, in particular in PFZ applications. In addition, by the integration of several characteristics with a number of mathematical representations, better climate patterns can be shown. We are therefore proposing the use of convolutionary networks since the influences are directed in the input vector to certain locations. This approach would enable the deeper network function maps to learn the links between input and IPFZ without having to look at all the characteristics of efficiency in PFZ variability.

The layer of pooling is added to reduce the display size. For each specified field, the supreme pooling layer chooses the greatest value, while the average layer chooses the average value. When creating the network model, each convolutionary layer was shadowed by a layer.

In classification applications, CNNs have been commonly used. Therefore, several activation functions were used to map the input functions in a number of categories. The output is measured as IPFZ in this investigation. This was why sigmoid (16) and hyperbolic tangent (17) were studied in the final layer, as they are non-linear activation functions.

$$\sigma(z) = \frac{1}{1+e^{-z}} \quad (16)$$

$$\sigma(z) = \frac{1}{1+e^{-z}} \quad (17)$$

If z is a summation of biased weights and layer, z = wk xk + b,wk is a weight of the connected layer, xk is a complete layer input, and b is bias, 1 ⩽ k ⩽ c, c are the weights and inputs of the fully connected layer. In this case, z is an input of the complete layer connector. Additional layers are frequently employed as flattening layers, converting the input into one dimension with multiple sizes. Usually drop-out is used to prevent overfitting. Usually the dataset is divided into training, validation and testing. The CNN training processes are shown

International Journal on Recent and Innovation Trends in Computing and Communication
ISSN: 2321-8169 Volume: 11 Issue: 2
DOI: https://doi.org/10.17762/ijritcc.v11i2.6131
***Article Received**: 18 December 2022 **Revised**: 12 January 2023 **Accepted**: 24 January 2023*

in algorithm 1. 1. During the training phase a number of functions might be deployed. As indicated in algorithm 1, a test point was provided to ensure better performance in the validation data set to preserve network weights

Algorithm 1: CNN Training Process

Input: Training and Validation dataset Output: Trained CNN
1: *Initialize the network weights and bias* 2: *For each epoch*: 3: *Process the records of the training data cases* 4: *Compare the actual values to predicted values* 5: *Calculate the loss function* 6: *Back propagate the error through the layers and adjust the network weights* 7: *Check the validation dataset* 8: *If better loss value obtained* 9: *Save the network weights* 10: *End* 11: *End* 12: *Return the trained CNN*

3.4.4. Ensemble Conditions

The condition will be applied to the CNN, PNN, and FFNN output labels, respectively, to arrive at the final decision label. Ensemble conditions are shown in Table 4.

Table 4: Ensemble Illness Table

FFNN Label	PNN Label	CNN Label	Final Decision Label
0	0	0	CNN
1	1	0	FFNN & PNN
1	1	1	FFNN, PNN & CNN
0	0	1	CNN
0	1	0	CNN
0	1	1	PNN & CNN
1	0	0	CNN
1	0	1	FFNN & CNN

When the output label value from all three networks (PNN, CNN, FFNN) is zero, the final decision label is taken from CNN. When the output label value from all three networks is one, the ML and DL techniques. When the PNN label is 1, the FFNN label is 1, and the CNN label is 1, with the other criteria (i.e. CNN-FFNN, PNN-CNN, and FFNN-PNN) set to zero, only the CNN label is chosen as final decision label. Once the FFNN label by itself is a 0, the PNN&CNN label is used to make the ultimate call. For similar reasons, when the CNN output label is 0, the FFNN&PNN label is taken as the final decision label, and vice versa when the PNN label alone is 0. The primary goal of this study is to use these final decision label values to forecast future IPFZ data with high accuracy.

IV. Results and Discussion

The suggested setup is being tested using MATLAB (version 2018a) on an Intel i5 CPU, with a 1TB hard drive, and 8GB of RAM.

A. Evaluation Metrics

Our approach's segmentation and classification capabilities are evaluated using the challenge assessment metrics. Measures of sensitivity (SE), specificity (SP), and false measure (FM) are used to assess segmentation performance. The following are the specifications for performance.

$$accuracy = (tp + tn)/N \quad (18)$$

$$sensitivity = tp\_rate \quad (19)$$

$$specificity = tn\_rate \quad (20)$$

$$precision = tp/(tp + fp) \quad (21)$$

$$recall = \frac{tp}{tp+fn} \quad (22)$$

$$f\_measure = 2 * ((precision * recall)/(precision + recall)) \quad (23)$$

$$gmean = sqrt(tp\_rate * tn\_rate) \quad (24)$$

N is the number of possible outcomes, where tp, tn, fp, and fn are the true positive, true negative, false positive, and false negative counts, correspondingly.

4.1. Performance Analysis of Projected CECT Procedure for the investigation of 80%-20% of available dataset

Here, we compare the CECT method's performance to that of the PNN method, the FFNN method, and the CNN method, checking its sensitivity, specificity, recall, precision, G-mean, accuracy, and F-measure along the way. this is the starting point for the analysis. Tabulated in Table 5 are the verified values for recall, precision, sensitivity, specificity, and g-mean that were obtained using the suggested CECT method..

Table 5: Performance Assessment of CECT Method for 80%-20% of obtainable dataset

Classification Technique	G-mean	Specificity	Precision	Sensitivity	Recall
PNN		0.8958	0.0884	1.0000	1.0000
FFNN	0.9465	0.9085	0.0994	1.0000	1.0000
CNN	0.9531	0.9258	0.1199	1.0000	1.0000
Proposed CECT Technique	0.9622	0.9400	0.1441	1.0000	1.0000

International Journal on Recent and Innovation Trends in Computing and Communication
ISSN: 2321-8169 Volume: 11 Issue: 2
DOI: https://doi.org/10.17762/ijritcc.v11i2.6131
***Article Received**: 18 December 2022 **Revised**: 12 January 2023 **Accepted**: 24 January 2023*

PNN, FFNN, CNN, and the suggested CECT approach all reach G-mean results of 94.65%, 95.31%, 96.22%, and 96.95%, respectively. Sensitivity is the inverse of recall, hence the examination of CNN, PNN, FFNN, and CECT techniques all yielded the same recall and sensitivity results (i.e.1.000). PNN, FFNN, CNN, and the proposed CECT all attained precisions of 0.08, 0.09, 0.11, and 0.14, respectively, demonstrating that the proposed CECT outperformed the individual ML and DL algorithms. Compared to the 89%, 90%, and 92% respective precisions attained by the PNN, FFNN, and CNN, the suggested CECT achieves a 94% precision. The foregoing experimental investigation showed that the suggested CECT outperformed CNN under the same experimental settings. Analyzing CECT's performance in terms of accuracy and f-measure is shown in Table 6 and Figure 8.

Table 6: Authentication of Projected CECT system for 80%-20% of obtainable dataset

Classification Technique	F-measure	Accuracy
PNN	0.1624	0.8969
FFNN	0.1808	0.9094
CNN	0.2140	0.9266
Projected CECT Technique	0.2520	0.9406

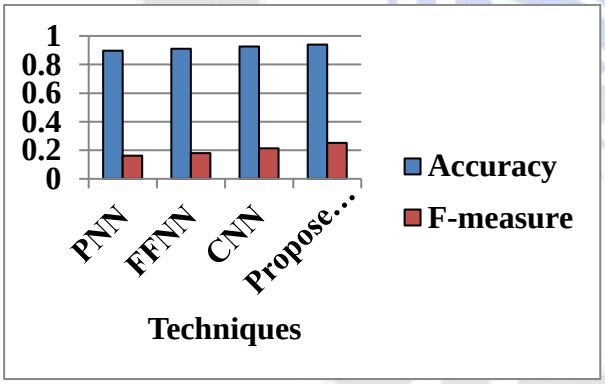

Figure 8: Graphical Representation of projected accuracy and F-measure

From the data shown in the table and figures above, it is evident that the suggested CECT approach outperformed the competition in terms of accuracy and f-measure. In terms of experimental accuracy, PNN, FFCNN, CNN, and the suggested CECT approaches all performed between 89% and 94%, respectively. All strategies produced f-measures of 0.16, 0.18, 0.21, and 0.25, respectively, demonstrating the superior performance of the suggested CECT methods. The experimental investigation of the suggested CECT using ML and DL methods for the analysis of 60%-40% in existing datasets follows.

4.2. Performance Analysis of Projected CECT Procedure for the analysis of 60%-40% of available dataset

To evaluate the efficacy of the suggested CECT methods, experiments are conducted utilizing 60% training data and 40% testing data to measure a variety of parameters. In terms of sensitivity, specificity, accuracy, recall, and G-mean, verified findings from a number of different methods are shown in Table 7.

Table 7: Performance Analysis of Projected CECT procedure for the 60%-40% of obtainable dataset

Classification Technique	Specificity	Sensitivity	Precision	G-mean	Recall
PNN	0.8169	1.0000	0.0523	0.9038	1.0000
FFNN	0.8674	1.0000	0.0708	0.9314	1.0000
CNN	0.8769	1.0000	0.0758	0.9364	1.0000
Proposed CECT Technique	0.9006	1.0000	0.0922	0.9490	1.0000

All four methods (PNN, FFNN, CNN, and the proposed CECT) obtained above 90% accuracy in the G-mean analysis (90.38%, 93.14%, 93.64%, and 94.90%, respectively). Comparing CNN, PNN, FFNN, and the CECT method yielded identical sensitivity and recall results (i.e.1.000). Precisions of 0.05, 0.07, 0.07, and 0.09 were reached by PNN, FFNN, CNN, and the proposed CECT, respectively; this demonstrates that the proposed CECT outperformed the individual ML and DL approaches. In comparison to the 81%, 86%, and 87% specificity reached by the PNN, FFNN, and CNN, respectively, the suggested CECT has a specificity of 90%. As can be seen from the above experimental study, the suggested CECT outperformed CNN thanks to the ensemble conditions that were applied to the ML and DL networks. However, the performance of CECT approach produced low performance. The reason for this is the divides of dataset. The accuracy and f-measure performance of the CECT method are analyzed in Table 8 and Figure 9.

Table 8: Experimental analysis of Proposed CECT method for the investigation of 60%-40% dataset

Classification Procedure	F-measure	Accuracy
PNN	0.0994	0.8187
FFNN	0.1322	0.8688
CNN	0.1410	0.8781
Proposed CECT Procedure	0.1689	0.9016

International Journal on Recent and Innovation Trends in Computing and Communication
ISSN: 2321-8169 Volume: 11 Issue: 2
DOI: https://doi.org/10.17762/ijritcc.v11i2.6131
***Article Received**: 18 December 2022 **Revised**: 12 January 2023 **Accepted**: 24 January 2023*

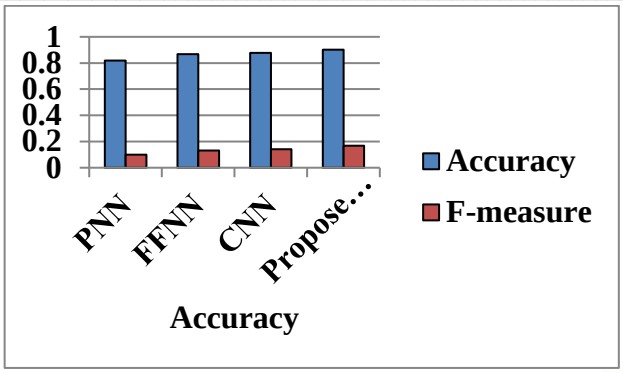

Figure 9: Graphical Illustration of projected CECT in terms of accuracy and F-measure

From the data shown in the table and figures above, it is evident that the suggested CECT approach outperformed the competition in terms of accuracy and f-measure. PNN, FFCNN, CNN, and the suggested CECT approaches all performed at 81%, 86%, 87%, and 90% accuracy in the studies. Although the suggested CECT approaches demonstrate greater performance than analysis of only 80%-20% of the dataset, their f-measures were only 0.09, 0.13, 0.14, and 0.16. In the following, we will demonstrate the experimental evaluation of the suggested CECT using ML and DL methods for the study of forthcoming data sets.

4.3. Performance Investigation of Projected CECT Procedure for the Future data prediction

Table 9 shows the validated results of various techniques in terms of sensitivity, specificity, precision, recall and G-mean for the future data.

Table 9: Validation of projected CECT Technique with ML and DL procedures for the future data analysis

Classification Technique	Specificity	G-mean	Precision	Sensitivity	Recall
PNN	0.5944		0.0243	1.0000	1.0000
FFNN	0.6449	0.7710	0.0277	1.0000	1.0000
CNN	0.6733	0.8030	0.0300	1.0000	1.0000
Proposed CECT Technique	0.7143	0.8205	0.0342	1.0000	1.0000

Acquiring accuracies of 0.02, 0.02, 0.03 and 0.034, respectively, in precision analyses were PNN, FFNN, CNN, and the new CECT method, respectively. Comparing CNN, PNN, FFNN, and the CECT method yielded identical sensitivity and recall results (i.e.1.000). The suggested CECT outperformed individual ML and DL methods, with a G-mean of 0.77, 0.80, 0.82, and 0.84 for PNN, FFNN, and CNN respectively. While the PNN, FFNN, and CNN all managed 59%, 64%, and 67%, respectively, the suggested CECT only managed 71% specificity. Results from the aforementioned experiments confirmed the superior performance of the proposed CECT compared to CNN and other ML methods. Future data requires more precise predictions, which may explain why CECT approach performed poorly when compared to analyses of 80%-20% and 60%-40% of the present dataset. The accuracy and f-measure results for CECT are shown in Table 10 and Figure 10, respectively.

Table 10: Validation of projected CECT Procedure in terms of accuracy and F-measure for the future data investigation

Classification Technique	Accuracy	F-measure
PNN	0.5984	0.0474
FFNN	0.6484	0.0538
CNN	0.6766	0.0582
Proposed CECT Technique	0.7172	0.0660

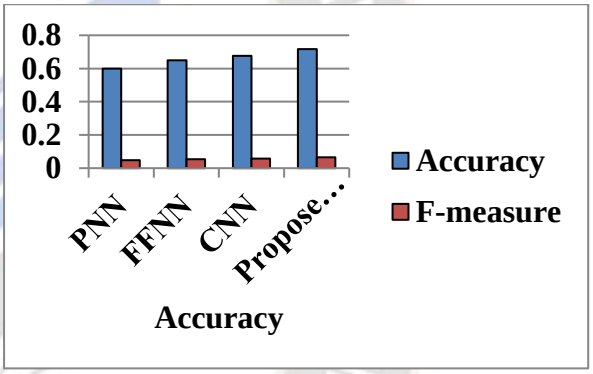

Figure 10: Graphical Illustration of projected CECT in terms of accuracy and F-measure

From the data shown in the table and figures above, it is evident that the suggested CECT approach outperformed the competition in terms of accuracy and f-measure. PNN, FFCNN, CNN, and the suggested CECT approaches all performed at or above 64%, 67%, and 71% respectively, in studies measuring accuracy. All strategies achieved f-measures of 0.04, 0.05, 0.05, and 0.06, demonstrating that the suggested CECT procedures exhibit superior performance than analysis of 80%-20% and 60%-40% of the dataset, respectively. Therefore, further development of the suggested CECT is required for reliable data projection into the future.

V. CONCLUSION

Modern ecology and conservation face significant challenges in the area of effective tracking of geographical distribution of varied human influences like fishing. While coastal fisheries in certain nations' national waters are monitored on a regular basis, the accuracy of fishing effort

International Journal on Recent and Innovation Trends in Computing and Communication
ISSN: 2321-8169 Volume: 11 Issue: 2
DOI: https://doi.org/10.17762/ijritcc.v11i2.6131
***Article Received**: 18 December 2022 **Revised**: 12 January 2023 **Accepted**: 24 January 2023*

maps for other regions, especially remote ones and the high seas, remains in question. It is imperative that fisheries management and conservation efforts be prioritized and implemented on a worldwide scale, but this cannot be done without first gaining a deeper understanding of the world's fishing fleets. Around 13–14 million people in India work in the fishing industry. The country has a marine coastline that extends for 7517 kilometers, 3,827 fishing villages, and 1,914 landing centers. Fish farmers in India only harvest an average of 2 tons per year on average. The level of living of Indian fishermen has the potential to rise thanks to high productivity, the transmission of knowledge for sustainable fishing, and the increase in fish exports. This project aims to address that issue and provide assistance to fishermen by identifying promising new fishing grounds. Pre-processing and normalization methods are used to the gathered data in order to eliminate missing values and other anomalies. Then, the necessary characteristics are extracted using a combination of 13 features and features derived from geometry and finance. Lastly, the requirements described in Table 4 are applied to the suggested CECT method for accurate prediction of the IPFZ. In order to compare the efficacy of the proposed CECT method with DL and ML, we conduct experiments. More than 93% accuracy was reached for 80%-20% using the suggested CECT method, while 71% accuracy was achieved for projected data analysis. The feature selection method combined with the CECT method is used for future IPFZ prediction.

REFERENCES

[1] Bradley, D.; Merrifield, M.; Miller, K.M.; LoMonico, S.; Wilson, J.R.; Gleason, M.G. Opportunities to improve fisheries management through innovative technology and advanced data systems. Fish Fish. 2019, 20, 564–583.

[2] Fosso, K.; Wamba, S.; Bawack, R.; Guthrie, C.; Queiroz, M.; Carillo, K. Are we preparing for a good AI society? A bibliometric review and research agenda. SSRN Electron. J. 2021, 164, 120482.

[3] Peeters, R.; Schuilenburg, M. The Algorithmic Society, Technology, Power, and Knowledge; Routledge: London, UK, 2021.

[4] Ossewaarde, M.; Gulenc, E. National Varieties of Artificial. Computer 2020, 53, 53–61.

[5] Mustafa, F.H. A Review of Smart Fish Farming Systems. J. Aquac. Eng. Fish. Res. 2016, 2, 193–200.

[6] Yang, X.; Zhang, S.; Liu, J.; Gao, Q.; Dong, S.; Zhou, C. Deep learning for smart fish farming: Applications, opportunities and challenges. Rev. Aquac. 2020, 13, 66–90.

[7] Pérez-Ortiz, M.; Fernández-Delgado, M.; Cernadas, E.; Domínguez-Petit, R.; Gutiérrez, P.A.; Hervás-Martínez, C. On the Use of Nominal and Ordinal Classifiers for the Discrimination of States of Development in Fish Oocytes. Neural Process. Lett. 2016, 44, 555–570.

[8] Li, K.; Sidorovskaia, N.A.; Tiemann, C.O. Model-based unsupervised clustering for distinguishing Cuvier's and Gervais' beaked whales in acoustic data. Ecol. Inform. 2020, 58, 101094.

[9] Raza, K.; Hong, S. Fast and Accurate Fish Detection Design with Improved YOLO-v3 Model and Transfer Learning. Int. J. Adv. Comput. Sci. Appl. 2020, 11, 7–16.

[10] Labao, A.B.; Naval, P.C. Cascaded deep network systems with linked ensemble components for underwater fish detection in the wild. Ecol. Inform. 2019, 52, 103–121.

[11] Siddiqui, S.A.; Salman, A.; Malik, M.I.; Shafait, F.; Mian, A.; Shortis, M.R.; Harvey, E.S. Automatic fish species classification in underwater videos: Exploiting pre-trained deep neural network models to compensate for limited labelled data. ICES J. Mar. Sci. 2018, 75, 374–389.

[12] Jalal, A.; Salman, A.; Mian, A.; Shortis, M.; Shafait, F. Fish detection and species classification in underwater environments using deep learning with temporal information. Ecol. Inform. 2020, 57, 101088.

[13] Chuaysi, B.; Kiattisin, S. Fishing Vessels Behavior Identification for Combating IUU Fishing: Enable Traceability at Sea. Wirel. Pers. Commun. 2020, 115, 2971–2993.

[14] Kylili, K.; Hadjistassou, C.; Artusi, A. An intelligent way for discerning plastics at the shorelines and the seas. Environ. Sci. Pollut. Res. 2020, 27, 42631–42643.

[15] Cantorna, D.; Dafonte, C.; Iglesias, A.; Arcay, B. Oil spill segmentation in SAR images using convolutional neural networks. A comparative analysis with clustering and logistic regression algorithms. Appl. Soft Comput. 2019, 84, 105716.

[16] Al-Ruzouq, R.; Gibril, M.; Shanableh, A.; Kais, A.; Hamed, O.; Al-Mansoori, S.; Khalil, M. Sensors, Features, and Machine Learning for Oil Spill Detection and Monitoring: A Review. Remote Sens. 2020, 12, 3338.

[17] Song, D.; Zhen, Z.; Wang, B.; Li, X.; Gao, L.; Wang, N.; Xie, T.; Zhang, T. A Novel Marine Oil Spillage Identification Scheme Based on Convolution Neural Network Feature Extraction from Fully Polarimetric SAR Imagery. IEEE Access 2020, 8, 59801–59820.

[18] Liu, S.; Liu, Y.; Alabia, I.D.; Tian, Y.; Ye, Z.; Yu, H.; Li, J.; Cheng, J. Impact of Climate Change on Wintering Ground of Japanese Anchovy (Engraulis japonicus) Using Marine Geospatial Statistics. Front. Mar. Sci. 2020, 7, 1–15.

[19] Cabreira, A.G., Martin Tripode and Adriain Madirolas "Artificial neural networks for fish-species identification, artificial neural networks for fish-species identification", ICES Journal of Marine Science, Vol.66, pp.1119–1129, 2009.

[20] Rodriguez,N., Orlando Duran " Multiscale Polynomial Autoregressive Model For Monthly Sardines Catches Forecasting" ,IEEE Fourth International Conference on Computer Sciences and Convergence Information Technology, 1524-1528, 2009.

International Journal on Recent and Innovation Trends in Computing and Communication
ISSN: 2321-8169 Volume: 11 Issue: 2
DOI: https://doi.org/10.17762/ijritcc.v11i2.6131
***Article Received**: 18 December 2022 **Revised**: 12 January 2023 **Accepted**: 24 January 2023*

[21] Shakya,S., Hongchun Yuan, Xinjun Chen and Liming Song "Application of Radial Basis Function Neural Network for Fishery Forecasting", IEEE, pp.287-291, 2011.

[22] Nurdin, S., Lihan, T. and Mustapha, A.M. "Mapping of Potential Fishing Grounds of Rastrelliger kanagurta (Cuvier, 1816) in the Archipelagic Waters of Spermonde Indonesia Using Satellite Images", Malaysia Geospatial Forum, Holiday Inn Melaka, pp.6-7, 2012.

[23] Salleh T Daqamseh, Shattri Mansor, Biswajeet Pradhan, Lawal Billa and Ahmad Rodzi Mahmud "Potential fish habitat mapping using MODIS-derived sea surface salinity, temperature and chlorophyll-a data: South China Sea Coastal areas, Malaysia", Geocarto International, Vol. First article, pp. 1–15, 2012.

[24] Tadjuddah,M., Ahmad Mustafa, Utama K. Pangerang and Farid Yasidi "Application of satellite multi-sensor techniques to detect upwellings and potential fishing grounds in Wakatobi Marine National Park, Southeast Sulawesi, Indonesia.", Aquatic Ecosystem Health and Management, Vol.15, No.3, pp.303–310, 2012.

[25] Parzen, E., 1962. On estimation of a probability density function and mode. The annals of mathematical statistics, 33(3), pp.1065-1076.

[26] Specht, D. F. (1990). Probabilistic neural networks. Neural networks, 3(1), 109-118.

[27] Rutkowski, D. T., & Kaufman, R. J. (2004). A trip to the ER: coping with stress. Trends in cell biology, 14(1), 20-28.